IDENTIFICATION AND CONTROL OF A UNMANNED GROUND VEHICLE BY USING ARDUINO

Marco C. DE SIMONE[1] and Domenico GUIDA[2]

In this paper, an identification activity and a control application conducted on a Unmanned Ground Vehicle by using low cost components and open source software are presented. The chassis of the vehicle is made of methyl methacrylate on which are mounted the wheel-motors group, the drives, and the ArduinoMega 2560 microcontroller. Furthermore, ultrasonic sensors and accelerometers are used for achieving the obstacle detection and for obtaining control signal feedback. The N4SID (Numerical algorithms for Subspace State Space System Identification) method was used to obtain a dynamical model of the unmanned vehicle, while open-loop and closed-loop control algorithms were implemented on the ArduinoMega controller. The results obtained in this investigation show the effectiveness of the proposed method for achieving the identification and control of mechanical systems.

Keywords: Identification, Control, Arduino, N4SID, UGV.

1. Introduction

In recent years we have witnessed the use of electric vehicles in many fields (e.g. agriculture, logistics, transport, ect.) [1, 2, 3, 4, 5]. The use of electric traction has made it easy to transform even complex vehicles into unmanned systems [6, 7]. Furthermore, researchers are focusing on the recovery of existing systems on the market, considered obsolete, which can be used again by retrofitting techniques, thereby reducing electronic waste production [8, 9, 10]. An autonomous vehicle or unmanned ground vehicle (UGV), uses its sensors to localise its position in the environment. Such information will be processed by the on-board controller, and, on the basis of the mission, it will properly manage its actuators [11, 12, 13]. For this reason, we decided to evaluate a procedure for identifying a dynamic model of a small robot on wheels [14, 15, 16, 17, 18, 19], and to design an optimal controller, in order to make the UGV follow desired trajectories [20, 21, 22, 23]. The paper is organized as follows. In section 2 we describe the unmanned vehicle used for the experimental activity. Section 3 focuses the attention on the set of equations

[1]Adj Professor, Dept.of Industrial Engineering, University of Salerno, Italy, mdesimone@unisa.it

[2]Full Professor, Dept.of Industrial Engineering, University of Salerno, Italy, guida@unisa.it

that describes a n DoF mechanical system and the performance index for a LQ optimal regulator, while section 4, reports the experimental activity conducted with the identification procedure and the design activity of the LQR controller by using a "state observer". Final section presents the conclusions. l

2. Description of the UGV

The unmanned ground vehicle reported in Fig. 1, is a small low weight three-wheeled robot with two fixed-axis wheel drive used for Identification and Control applications. The chassis of the vehicle is made of methyl methacrylate. The two motorized wheels are driven by DC electric gear-motors with digital incremental encoders. Each pair of motors is powered by a drive. Sensors

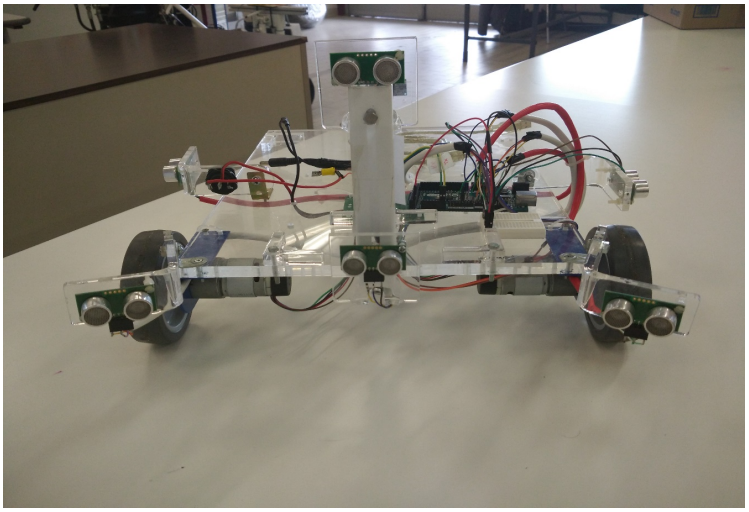

FIGURE 1. Unmanned Ground Vehicle

and actuators are all connected to the ArduinoMega2560 controller. Sensors, actuators and micro-controller are powered by a 12 Volts battery as shown in Fig. 2. On the vehicle are present ultrasonic sensors for detecting the presence of obstacles along the trajectory, a triple-axis accelerometer, a triple-axis gyroscope and a triple-axis magnetometer for a total of eleven transducers. The 12 volts battery is the heaviest component installed on the chassis and contributes by two-thirds to the total weight of the robot that is about 3 kg. The Arduino Mega 2560 board is a microcontroller based on the ATmega2560 processor. Such controller has digital and analogic I/O ports that allow to collect data from any type of sensor and govern different types of actuators [24]. In Fig. 3, we have reported the on-board hardware operation scheme. The microcontroller, by means of a PWM signals, provides information to the DC motors drive to adjust the supplied voltage to the actuators. The MD25 drive is directly connected to the 12 volts on-board battery and supplies the power to the DC motors and ultrasonic sensors SRF05. The EMG30 is a 12

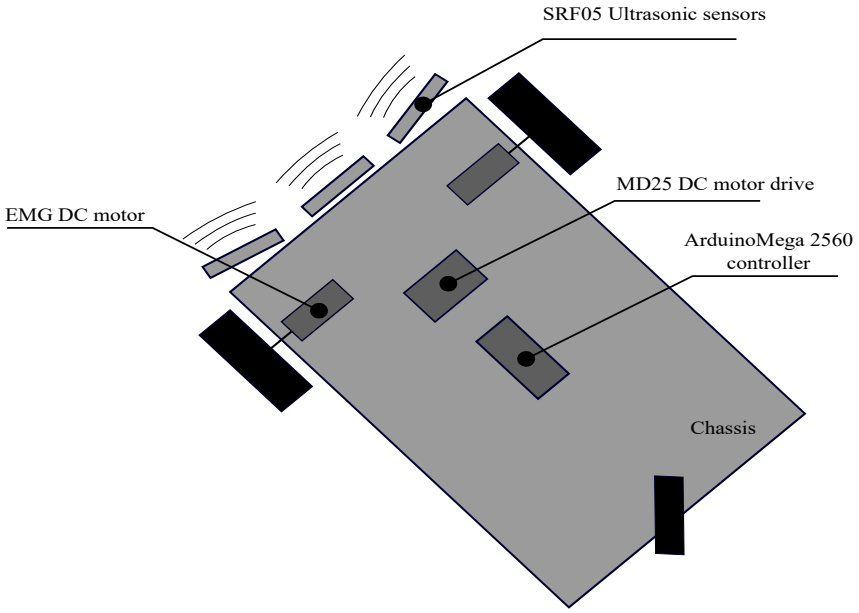

FIGURE 2. Scheme of the UGV with Onboard Main Components

volts motor fully equipped with encoders and a 30:1 reduction gearbox. It is ideal for small or medium robotic applications, providing cost effective drive and feedback for the user. It also includes a standard noise suppression capacitor across the motor windings. The wheels are directly connected on the drive shaft of the gearbox. The encoders feedback to the drive information about the revolutions of the wheels that is send finally to the microcontroller for trajectory evaluation, with a good approximation in case of slow dynamics.

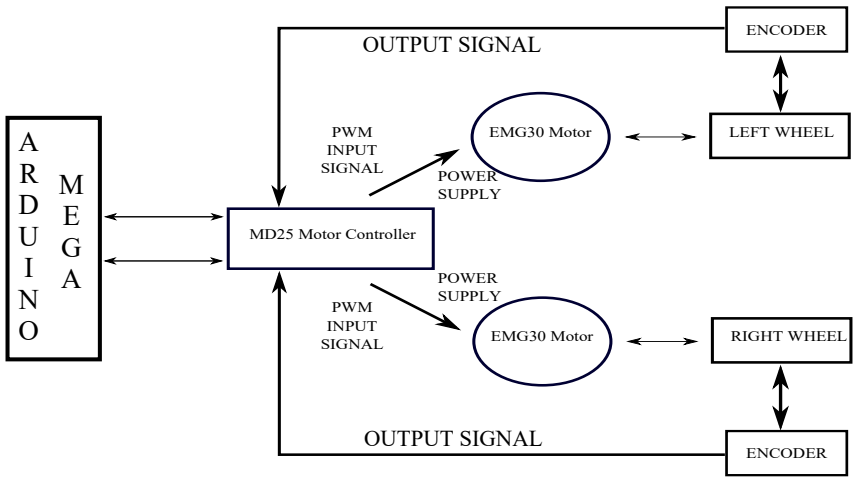

FIGURE 3. Bloc Representation of UGV

3. Mathematical Model

3.1. State-Space model

The equations of motion for a finite-dimensional linear (or linearised) dynamic system are a set of n_2 second-order differential equations, where n_2 is the number of independent coordinates:

$$\mathbf{M}\ddot{\mathbf{x}}(t) + \mathbf{R}\dot{\mathbf{x}}(t) + \mathbf{K}\mathbf{x}(t) = \mathbf{F}(t). \tag{1}$$

where $\mathbf{M}$, $\mathbf{R}$ and $\mathbf{K}$ are the mass, damping and stiffness matrices, and $\ddot{\mathbf{x}}(t)$, $\dot{\mathbf{x}}(t)$ and $\mathbf{x}(t)$ are vectors of generalised acceleration, velocity and displacement, respectively. Furthermore, with $\mathbf{F}(t)$ we denoted the forcing function. On the other hand, if the response of the dynamic system is measured by the m output quantities in the output vector $\mathbf{y}(t)$, then the output equations can be written in a matrix form as follows:

$$\mathbf{y}(t) = \mathbf{C_a}\ddot{\mathbf{x}}(t) + \mathbf{C_v}\dot{\mathbf{x}}(t) + \mathbf{C_d}\mathbf{x}(t). \tag{2}$$

where $\mathbf{C_a}$, $\mathbf{C_v}$ and $\mathbf{C_d}$ are output influence matrices for acceleration, velocity and displacement, respectively. These output influences matrices describe the relation between the vectors $\ddot{\mathbf{x}}(t)$,$\dot{\mathbf{x}}(t)$,$\mathbf{x}(t)$ and the measurement vector $\mathbf{y}(t)$. Let $\mathbf{z}(t)$ be the state vector of the system:

$$\mathbf{z}(t) = \begin{bmatrix} \mathbf{x}(t) \\ \dot{\mathbf{x}}(t) \end{bmatrix}, \tag{3}$$

if the excitations of the dynamic system is measured by the r input quantities in the input vector $\mathbf{u}(t)$, the equations of motions and the set of output equations can both be respectively rewritten in terms of the state vector as follows:

$$\begin{aligned} \dot{\mathbf{z}}(t) &= \mathbf{A_c}\mathbf{z}(t) + \mathbf{B_c}\mathbf{u}(t), \\ \mathbf{y}(t) &= \mathbf{C}\mathbf{z}(t) + \mathbf{D}\mathbf{u}(t). \end{aligned} \tag{4}$$

where $\mathbf{A_c}$ is the state matrix, $\mathbf{B_c}$ is the state influence matrix, $\mathbf{C}$ is the measurement influence matrix and $\mathbf{D}$ is the direct transmission matrix. These matrices can be computed in this way:

$$\mathbf{A_c} = \begin{bmatrix} \mathbf{0} & \mathbf{I} \\ -\mathbf{M}^{-1}\mathbf{K} & -\mathbf{M}^{-1}\mathbf{R} \end{bmatrix}. \tag{5}$$

$$\mathbf{B_c} = \begin{bmatrix} \mathbf{0} \\ \mathbf{M}^{-1}\mathbf{B_2} \end{bmatrix}. \tag{6}$$

$$\mathbf{C} = \begin{bmatrix} \mathbf{C_d} - \mathbf{C_a}\mathbf{M}^{-1}\mathbf{K}\mathbf{C_v} & -\mathbf{C_a}\mathbf{M}^{-1}\mathbf{R} \end{bmatrix}. \tag{7}$$

$$\mathbf{D} = \mathbf{C_a}\mathbf{M}^{-1}\mathbf{B_2}. \tag{8}$$

where $\mathbf{B_2}$ is an influence matrix characterising the locations and the type of inputs according to this equation:

$$\mathbf{F}(t) = \mathbf{B_2}\mathbf{u}(t). \tag{9}$$

In the case, very common, in which the measured output is just a linear combination of the state, the output equation becomes:

$$\mathbf{y}(t) = \mathbf{C}\mathbf{z}(t). \tag{10}$$

The equations (4) and (10) constitute a continuous-time state-space model of a dynamical system. On the other hand, considering a discrete-time state-space model of a dynamical system, (4) and (10) can be rewritten in the following way:

$$\begin{aligned} \mathbf{z}(k+1) &= \mathbf{A}\mathbf{z}(k) + \mathbf{B}\mathbf{u}(k), \\ \mathbf{y}(k) &= \mathbf{C}\mathbf{z}(k). \end{aligned} \tag{11}$$

Because experimental data are discrete in nature, the equations (11) form the basis for the system identification of linear, time-invariant, dynamical systems. The state matrix $\mathbf{A}$ and the influence matrix $\mathbf{B}$ of the discrete-time model can be computed from the analogous matrices $\mathbf{A_c}$, $\mathbf{B_c}$ of the continuous-time model sampling the system at equally spaced intervals of time:

$$\mathbf{A} = e^{\mathbf{A_c}\Delta t}, \qquad \mathbf{B} = \int_0^{\Delta t} e^{\Delta_c \tau} d\tau \mathbf{B_c}. \tag{12}$$

where Δt constant interval.

3.2. LQ Optimal Regulation

In optimal control one attempts to find a controller that provides the best possible performance with respect to some given index of performance. E.g., the controller that uses the least amount of control-signal energy to take the output to zero [25, 26, 27, 28]. In this case the performance index would be the control-signal energy. When the mathematical model of the system to be controlled is linear and the functions that appear in the index of performance have a quadratic form, we have a problem of LQ optimal control. Considering the linear model stationary, stabilizable and detectable, reported in (11),the problem of regulation (LQ) in infinite time is to determine the optimal feedback control law which minimises the performance index:

$$J_{LQ} := \sum_{k=1}^{\infty} \left[\mathbf{y}^T(k)\mathbf{Q}\mathbf{y}(k) + \mathbf{u}^T(k)\mathbf{R}\mathbf{u}(k) \right]. \tag{13}$$

where $\mathbf{Q} = \mathbf{Q}^T > 0$ and $\mathbf{R} = \mathbf{R}^T$.
The following equation corresponds to the energy of the control signal:

$$\sum_{k=1}^{\infty} \mathbf{u}^T(k)\mathbf{R}\mathbf{u}(k). \tag{14}$$

while the energy of the controlled output is expressed in (15)

$$\sum_{k=1}^{\infty} \mathbf{y}^T(k)\mathbf{Q}\mathbf{y}(k). \tag{15}$$

The solution is given by the control law:

$$\mathbf{u}(k) = -\mathbf{K}\mathbf{z}(k), \qquad \mathbf{K} = \mathbf{R}^{-1}\mathbf{B}^T\mathbf{S} \tag{16}$$

where the symmetric matrix S is the unique positive semidefinite solution of the *algebric Riccati equation* (ARE). The matrix $\mathbf{Q}$ and $\mathbf{R}$, in order to penalise more the non-zero position, can be chosen by applying the following rule:

$$Q_{ii} = \frac{1}{\text{maximum acceptable value of } y_i^2} \tag{17}$$

$$R_{ii} = \frac{1}{\text{maximum acceptable value of } u_i^2} \tag{18}$$

3.3. State-Space Observer Model

As seen in section 3.2 the optimal solution of a regulation problem (LQ), consists in the feedback of the state variables of the model of the system to be controlled. Often, however, the state variables of the system are not directly measurable. For this reason, it becomes essential in the design of a control system, to use of a state observer in order to estimate the state. These devices allow to obtain an estimate of the state variables from the knowledge of past inputs and measures available of the system. The observer of the state, must have in order to be acceptable, two fundamental properties. By denoting with $\mathbf{z}(k)$ the true state, with $\hat{\mathbf{z}}(k)$ the predicted state and $\mathbf{e}(k) := \mathbf{z}(k) - \hat{\mathbf{z}}(k)$ the estimates error, we can assert that the estimation error should converge to zero for $k \to \infty$ with the convergence speed that can be arbitrarily set by the control designer. Considering the following linear system, stationary and fully observable:

$$\begin{aligned} \mathbf{z}(k+1) &= \mathbf{A}\mathbf{z}(k) + \mathbf{B}\mathbf{u}(k), \qquad \mathbf{z}(k=1) = \mathbf{z}_0 \\ \mathbf{y}(k) &= \mathbf{C}\mathbf{z}(k). \end{aligned} \tag{19}$$

Lets suppose that the system is of order n and the output vector is of dimension m with $m < n$, and that the initial state $\mathbf{z}_0$ is not known. Our intention is to build a state estimator for the system (19) of the form:

$$\hat{\mathbf{z}}(k+1) = \mathbf{A}\hat{\mathbf{z}}(k) + \mathbf{B}\mathbf{u}(k) + \mathbf{G}\left[\mathbf{y}(k) - \mathbf{C}\hat{\mathbf{z}}(k)\right], \qquad \hat{\mathbf{z}}(k=1) = \hat{\mathbf{z_0}}. \tag{20}$$

i.e. using the error on the estimate of the extent to modify the behaviour of the observer. The above equation can also be written as:

$$\hat{\mathbf{z}}(k+1) = (\mathbf{A} - \mathbf{G}\mathbf{C})\,\hat{\mathbf{z}}(k) + \mathbf{B}\mathbf{u}(k) + \mathbf{G}\mathbf{y}(k), \qquad \hat{\mathbf{z}}(k=1) = \hat{\mathbf{z_0}}. \tag{21}$$

From (19) and (20) it is possible to derive the following model of the estimation error:

$$\hat{\mathbf{e}}(k+1) = (\mathbf{A} - \mathbf{G}\mathbf{C})\,\hat{\mathbf{e}}(k) \qquad \mathbf{e}(k=1) = \mathbf{z_0} - \hat{\mathbf{z_0}}, \tag{22}$$

from which it follows that, in order to make effective the estimate,we must choose the eigenvalues of $\mathbf{A} - \mathbf{G}\mathbf{C}$ with negative real part sufficiently lower than the smallest real part of the eigenvalues of the matrix A. Since the system (19), is fully observable, it is always possible to determine the matrix $\mathbf{K}$ in such

a way that the matrix $\mathbf{A} - \mathbf{GC}$ has arbitrary eigenvalues. The matrix $\mathbf{G}$ is called the gain matrix of the observer. The speed with which it extinguishes the error depends on the dynamics of the observer and thus is greater as much as is big (in form) the real part (negative) of the eigenvalues of the matrix $\mathbf{A} - \mathbf{GC}$.

4. Experimental activity

A multi-body model of the UGV has been developed for calculating feed-forward control laws [29, 30, 31]. Then, it has been developed an experimental activity to verify the theoretical feed-forward law [32, 33, 34]. It has been observed that the feedforward control is sensible to noise [35, 36, 37]., To make robust the control law it has been developed an identification procedure for obtaining the state matrix and the state observer(see (20)). This procedure is based on N4SID method. On the basis of identified system it has been developed an LQ regulator that has been added to feed-forward control in order to make more effective the control system.

4.1. Identification procedure

In this paper we used N4SID method for the identification of the system. N4SID numerical method allows to obtain the state matrix and the state observer by input-output data [38, 39, 40, 41]. The state space matrices are not calculated in their canonical forms (with a minimal number of parameters), but as full state space matrices in a certain, almost optimally conditioned basis (this basis is uniquely determined, so that there is no problem of identifiability). This implies that the observability (or controllability) indices do not have to be known in advance. Input and output data, indicated in Fig. 4, formed by voltage applied to the DC motors and angular rotation of the wheels, are fed to the algorithm N4SID, in order to calculate the matrices $\mathbf{A}$,$\mathbf{B}$,$\mathbf{C}$,$\mathbf{D}$ and the observer matrix $\mathbf{G}$. These matrices have been obtained assuming the sampling period of the input and output equal to $T_s = 0.01$ s. The delay between the input motor signals and the output rotation of the wheels signal, is due to the translational and rotational inertia of the entire system.

$$A = \begin{bmatrix} 1 & -4.740e-05 & 2.665e-06 & -3.708e-05 \\ -0.0005266 & 1.001 & -0.01689 & 0.0006557 \\ 0.001857 & 0.01783 & 0.9946 & -0.01416 \\ 0.001423 & 0.003359 & 0.008817 & 0.9834 \end{bmatrix}. \tag{23}$$

$$B = \begin{bmatrix} -1e-07 & -4.574e-08 \\ 2.537e-05 & -5.01e-0.5 \\ -1.4e-05 & -2.524e-05 \\ 0.0001159 & -4.996e-05 \end{bmatrix}. \tag{24}$$

$$C = \begin{bmatrix} 1.263e+05 & -461.7 & 4.65 & -2.088 \\ 9.051e+04 & 663.9 & -3.721 & -0.5209 \end{bmatrix}. \tag{25}$$

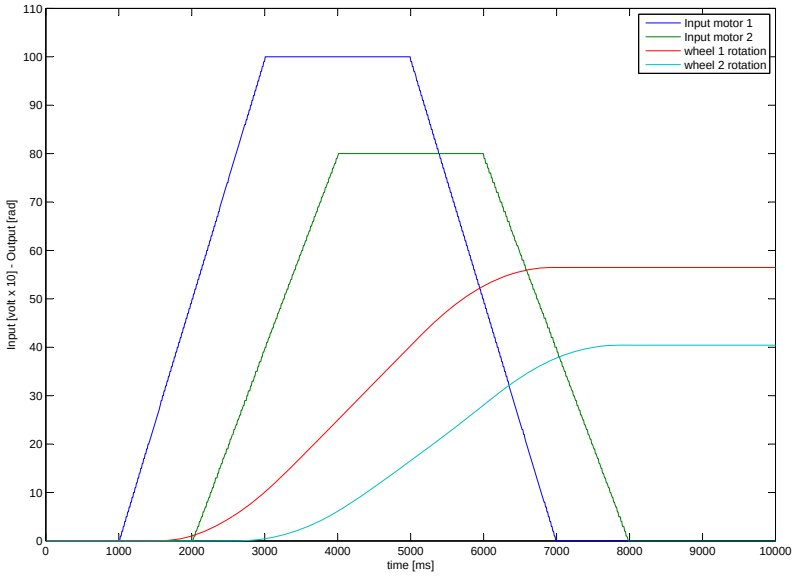

FIGURE 4. Input and Output Signals

$$D = \begin{bmatrix} 0 & 0 \\ 0 & 0 \end{bmatrix} \tag{26}$$

$$G = \begin{bmatrix} 2.215e-06 & 1.565e-06 \\ -3.385e-04 & 4.117e-04 \\ 0.0049 & -0.0067 \\ -0.0108 & -0.0037 \end{bmatrix} \tag{27}$$

4.2. LQR Control

To the feed-forward control is added a feed-back compensator that is proportional to the deviation $\delta\hat{\mathbf{z}}(k) = \hat{\mathbf{z}}(k) - \overline{\mathbf{z}}(k)$:

$$\delta\mathbf{u}(k) = -\mathbf{K}\delta\hat{\mathbf{z}}(k) \tag{28}$$

where $\hat{\mathbf{z}}$ is the estimated state and $\overline{\mathbf{z}}$ is the imposed state, respectively. The equation used for estimating the deviation, similar to (20) is reported below:

$$\delta\hat{\mathbf{z}}(k+1) = \mathbf{A}\delta\hat{\mathbf{z}}(k) + \mathbf{B}\delta\mathbf{u}(k) + \mathbf{G}\left[\delta\mathbf{y}(k) - \delta\hat{\mathbf{y}}(k)\right]. \tag{29}$$

with

$$\delta\hat{\mathbf{y}}(k) = \mathbf{C}\delta\hat{\mathbf{z}}(k). \tag{30}$$

in which $\delta\hat{\mathbf{y}}(k) = \hat{\mathbf{y}}(k) - \overline{\mathbf{y}}(t)$ and $\delta\mathbf{y}(k) = \mathbf{y} - \overline{\mathbf{y}}$, where $\hat{\mathbf{y}}$ is estimated output, $\overline{\mathbf{y}}$ is the imposed output and $\mathbf{y}$ is the actual output. The state matrix $\mathbf{A}$, the input matrix $\mathbf{B}$, the output $\mathbf{C}$, the feed-forward matrix $\mathbf{D}$ and the observer matrix $\mathbf{G}$ are reported in (23),(24),(25),(26) and (27). The control gain matrix

K has been calculated by applying LQR optimal control method in which the penalisation matrices **Q** and **R** are the following:

$$\mathbf{Q} = \begin{bmatrix} \frac{1}{100^2} & 0 \\ 0 & \frac{1}{100^2} \end{bmatrix}, \qquad \mathbf{R} = \begin{bmatrix} \frac{1}{100^2} & 0 \\ 0 & \frac{1}{100^2} \end{bmatrix} \tag{31}$$

In this way, we obtained the following matrix **K**:

$$\mathbf{K} = \begin{bmatrix} -1.5119e+05 & 444.8 & -81,875 & 136.34 \\ 1.2608e+04 & -650.39 & 87.417 & -9.2388 \end{bmatrix} \tag{32}$$

In fig. 5 are indicated the three UGV trajectories followed by the vehicle in

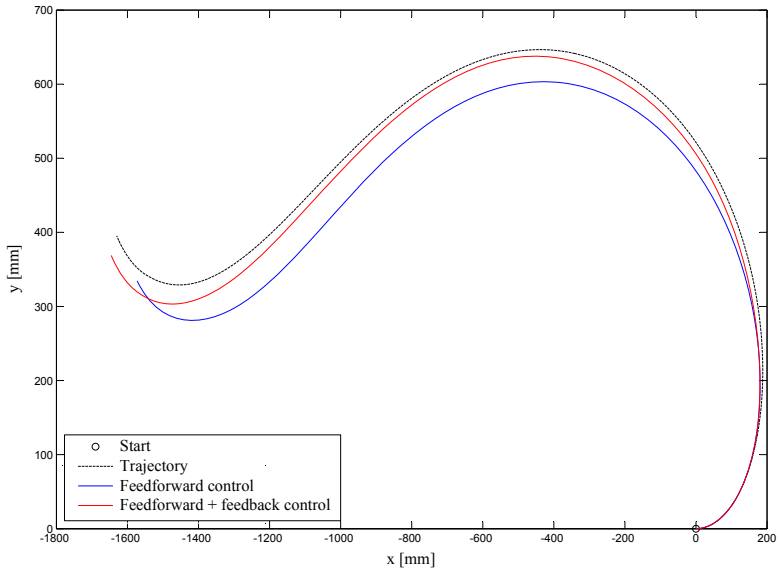

FIGURE 5. Target, FFC, FFC + FBC trajectory of the UGV

this activity. By the black line, it is indicated the chosen target trajectory while, by the blue line, we indicated the UGV trajectory obtained by means a feed-forward control law. Finally, by the red line, the trajectory followed by the unmanned vehicle, by applying to the DC motors the feed-forward and the feedback control law calculated by means an identification procedure. In fig. 6, the DC motor inputs are reported for evaluated feed-forward control law by the blue and green line, while with the black and red line, the feed-forward together with the feed-back control law, respectively

5. Conclusions

The research efforts of the authors are focused on the development of new methods [42, 43, 44, 45, 46, 47, 48, 49] ,for obtaining analytic models employing experimental data and optimal control strategies for rigid-flexible multi-body mechanical systems [50, 51, 52, 53, 54]. In this paper, an experimental activity has been conducted on a unmanned ground vehicle (UGV),

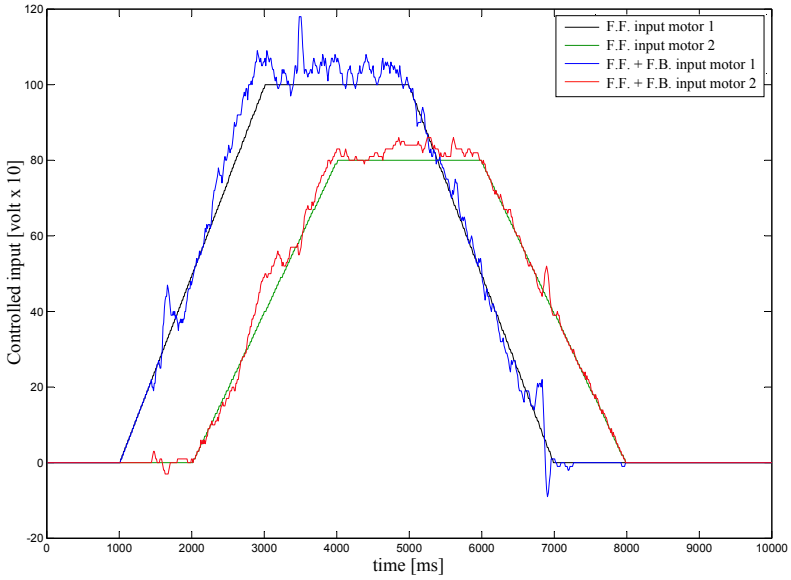

FIGURE 6. Motor Inputs

a small three-wheeled robot with two fixed-axis wheel drive. The vehicle is equipped with electric gear DC motors and ultrasonic sensors for obstacles detection. Gps sensor and inertia measurement unit (IMU) are also present on the vehicle for dead reckoning activities. The chassis of the unmanned vehicle is made of methyl-methacrylate. The identification method used for estimating the state space equations of motion of the system is the subspace state space system identification (N4SID) of Matlab software, by means of input and output experimental data. The input signal is the Voltage given to the left and right DC motor by the micro-controller ArduinoMega 2560 [55, 56, 57]. The EMG30 DC gear-motor is equipped with digital incremental encoders that measure the angular rotation of the gear motors axis, rotation used as output data for such activity. The N4SID algorithm gave us the possibility to evaluate the four state-space matrices. Due to the impossibility to measure all of the state of the system (i.e. only the angular rotation is measurable), a state observer is needed to estimate the system state. Such estimated state is used for the LQR control law design by imposing the two penalization matrices. In summary, the feed-forward control law, obtained by using a multi-body model of the vehicle can not be effective for imposing the target trajectory, due to noise and parameter uncertainty [58, 59, 60, 61]. In order to overcome this drawback, by using N4SID algorithm, an identified model of the system has been used for designing the LQ regulator in order to make the UGV follow the target trajectory. The experimental results have proved the goodness of such procedure.

REFERENCES

[1] *M. C. De Simone, S. Russo, Z. B. Rivera and D. Guida*, (2017). Multibody Model of a UAV in Presence of Wind Fields, ICCAIRO-2017 International Conference on Control, Artificial Intelligence, Robotics and Optimization, Prague, Czech Republic, 20-22 May 2017.

[2] *K. A. M. Annuar, M. H. M. Zin, M. H. Harun, M. F. M. A. Halim, and A. H. Azahar*, Design and development of search and rescue robot, International Journal of Mechanical and Mechatronics Engineering, 2016, 16(2), pp. 36–41.

[3] *M. Uma Maheswari and D. Rajalakshmi*, Arduino based robotic implementation of adaptive cruise control system, International Journal of Applied Engineering Research, 2015, 10(20), pp. 18409–18414.

[4] *C. M. Pappalardo, M. Patel, B. Tinsley and A. A. Shabana*, Pantograph/Catenary Contact Force Control, Proceedings of the ASME 2015 International Design Engineering Technical Conferences and Computers and Information in Engineering Conference IDETC/CIE 2015, Boston, Massachusetts, USA, August 2-5, 2015, pp. 1-11.

[5] *S. Kulkarni, C. M. Pappalardo and A. A. Shabana*, Pantograph/Catenary Contact Formulations, ASME Journal of Vibrations and Acoustics, 2017, 139(1), 011010.

[6] *A. Concilio, M. C. De Simone, Z. B. Rivera and D. Guida*, A New Semi-active Suspension System For Racing Vehicles, FME Transactions, 2017, 45(4), pp. 578-584.

[7] *P. Corke*, Robotics, Vision and Control, Springer Tracts in Advanced Robotics, 2nd ed, 2013.

[8] *A. Quatrano, M. C. De Simone, Z. B. Rivera and D. Guida*, Development and Implementation of a Control System for a retrofitted CNC Machine by using Arduino, FME Transactions, 2017, 45(4), pp. 565-571.

[9] *A. Ruggiero, M. C. De Simone, D. Russo, and D. Guida*, Sound pressure measurement of orchestral instruments in the concert hall of a public school, International Journal of Circuits, Systems and Signal Processing, 2016, 10, pp. 75-812.

[10] *C. M. Pappalardo, M. D. Patel, B. Tinsley and A. A. Shabana*, Contact Force Control in Multibody Pantograph/Catenary Systems, Proceedings of the Institution of Mechanical Engineers, Part K: Journal of Multibody Dynamics, 2016, 230(4), pp. 307-328.

[11] *Y. Wang, A. Goila, R. Shetty, M. Heydari, A. Desai and H. Yang*, Obstacle Avoidance Strategy and Implementation for Unmanned Ground Vehicle Using LIDAR, SAE International Journal of Commercial Vehicles, 2017, 10(1), pp. 50–55.

[12] *R. Velrajkumar, E. Murthy, E. Raja, J. Hossen and L. K. Jong*, Controlling and tracking of mobile robot in real-time using android platform, Journal of Engineering and Applied Sciences, 2017, 12(4), pp. 929–932.

[13] *G. Lockridge, B. Dzwonkowski, R. Nelson and S. Powers*, Development of a low-cost arduino-based sonde for coastal applications, Sensors (Switzerland), 2016, 16(4),4.

[14] *A. Goncalves Costa Junior, J. Antonio Riul P. Henrique Miranda Montenegro*, Application of the Subspace Identification Method using the N4SID Technique for a Robotic Manipulator, IEEE Latin America Transactions, 2016, 14(4), pp. 1588–1593.

[15] *T. Ba, X. Guan and J. Zhang*, Vehicle lateral dynamics modelling by subspace identification methods and tyre cornering stiffness estimation, International Journal of Vehicle Systems Modelling and Testing, 2015, 10(4), pp. 340-355.

[16] *A. Formato, D. Ianniello, F. Villecco, T. L. L. Lenza, and D. Guida*, Design Optimization of the Plough Working Surface by Computerized Mathematical Model, Emirates Journal of Food and Agriculture, 2017, 29(1), pp. 36-44.

[17] *D. Guida, F. Nilvetti and C. M. Pappalardo*, Parameter Identification of a Two Degrees of Freedom Mechanical System, International Journal of Mechanics, 2009, 3(2), pp. 23–30.

[18] *D. Guida, F. Nilvetti and C. M. Pappalardo*, On Parameter Identification of Linear Mechanical Systems, Programme and Proceedings of 3rd International Conference on Applied Mathematics, Simulation, Modelling (ASM'09), Vouliagmeni Beach, Athens, Greece, December 2009, 29–31, pp. 55-60.

[19] *P. Van Overschee and B. L. De Moor*. Subspace identification for linear systems: TheoryImplementationApplications. Springer Science & Business Media, 2012.

[20] *D. Guida and C. M. Pappalardo*, Control Design of an Active Suspension System for a Quarter-Car Model with Hysteresis, Journal of Vibration Engineering and Technologies, 2015, 3(3), pp. 277-299.

[21] *D. Guida, F. Nilvetti and C. M. Pappalardo*, Optimal Control Design by Adjoint-Based Optimization for Active Mass Damper with Dry Friction, Programme and Proceedings of COMPDYN 2013 4th International Conference on Computational Methods in Structural Dynamics and Earthquake Engineering, Kos Island, Greece, June 12-14, 2013, pp. 1–19.

[22] *A. E. Bryson*, Applied optimal control: optimization, estimation and control. CRC Press, 1975.

[23] *K. Zhou, J. C. Doyle and K. Glover*, Robust and optimal control (Vol. 40, p. 146). New Jersey: Prentice hall, 1996.

[24] *M. C. De Simone and D. Guida*, On the Development of a Low Cost Device for Retrofitting Tracked Vehicles for Autonomous Navigation, Programme and Proceedings of the XXIII Conference of the Italian Association of Theoretical and Applied Mechanics (AIMETA 2017), 4-7.09.2017, Salerno, Italy, 2017, pp. 71–82

[25] *P. Sena, P. Attianese, M. Pappalardo, and F. Villecco*, FIDELITY: Fuzzy Inferential Diagnostic Engine for on-LIne supporT to phYsicians, in 4th International Conference on Biomedical Engineering in Vietnam, Springer Berlin Heidelberg, 2013, pp. 396-400.

[26] *D. Guida, F. Nilvetti and C. M. Pappalardo*, Adjoint-based Optimal Control Design for a Cart Pendulum System with Dry Friction, Programme and Proceedings of ECCOMAS Thematic Conference on Multibody Dynamics, Zagreb, Croatia, July 1-4, 2013, pp. 269–285.

[27] *C. M. Pappalardo and D. Guida*, D., Control of Nonlinear Vibrations using the Adjoint Method, Meccanica, 2017, 52(11-12), pp. 2503-2526.

[28] *C. M. Pappalardo and D. Guida*, Adjoint-based Optimization Procedure for Active Vibration Control of Nonlinear Mechanical Systems, ASME Journal of Dynamic Systems, Measurement, and Control, 2017, 139(8), 081010.

[29] *C. M. Pappalardo and D. Guida*, Dynamic Analysis of Planar Rigid Multibody Systems modeled using Natural Absolute Coordinates, Applied and Computational Mechanics, Accepted for publication.

[30] *C. M. Pappalardo*, A Natural Absolute Coordinate Formulation for the Kinematic and Dynamic Analysis of Rigid Multibody Systems, Nonlinear Dynamics, 2015, 81(4), pp. 1841-1869.

[31] *P. Sena, P. Attianese, F. Carbone, A. Pellegrino, A. Pinto, and F. Villecco*, A Fuzzy Model to Interpret Data of Drive Performances from Patients with Sleep Deprivation, Computational and Mathematical Methods in Medicine, 2012.

[32] *D. Guida, F. Nilvetti and C. M. Pappalardo*, Dry Friction Influence on Cart Pendulum Dynamics", International Journal of Mechanics, 2009, 3(2), pp. 31–38.

[33] *D. Guida, F. Nilvetti and C. M. Pappalardo*, Dry Friction Influence on Inverted Pendulum Control, Programme and Proceedings of 3rd International Conference on Applied Mathematics, Simulation, Modelling (ASM'09), Vouliagmeni Beach, Athens, Greece, December 29-31, 2009, pp. 49–54.

[34] *D. Guida, F. Nilvetti and C. M. Pappalardo*, On the use of Two-dimensional Euler Parameters for the Dynamic Simulation of Planar Rigid Multibody Systems, Archive of Applied Mechanics, 87(10), pp. 1647-1665.

[35] *D. Guida, F. Nilvetti and C. M. Pappalardo*, Friction Induced Vibrations of a Two Degrees of Freedom System, Programme and Proceedings of 10th WSEAS International Conference on Robotics, Control and Manufacturing Technology (ROCOM '10), Hangzhou, China, April 11–13, 2010, pp. 133-136.

[36] *M. C. De Simone and D. Guida*, Dry Friction Influence on Structure Dynamics, COMPDYN 2015 - 5th ECCOMAS Thematic Conference on Computational Methods in Structural Dynamics and Earthquake Engineering, 2015, pp. 4483–4491.

[37] *D. Guida, F. Nilvetti and C. M. Pappalardo*, Instability Induced by Dry Friction, International Journal of Mechanics, 2009, 3(3), pp. 44–51.

[38] *J. N. Juang and M. Q. Phan*, Identification and control of mechanical systems. Cambridge University Press, 2004.

[39] *P. Van Overschee and B. De Moor*, N4SID: Subspace algorithms for the identification of combined deterministic-stochastic systems. Automatica, 1994, 30.1: pp. 75-93.

[40] *D. Guida and C. M. Pappalardo*, , 2009, "Sommerfeld and Mass Parameter Identification of Lubricated Journal Bearing", WSEAS Transactions on Applied and Theoretical Mechanics, 4(4), pp. 205–214.

[41] *D. Guida, F. Nilvetti and C. M. Pappalardo*, , 2011, "Mass, Stiffness and Damping Identification of a Two-story Building Model", Programme and Proceedings of rd ECCOMAS Thematic Conference on Computational Methods in Structural Dynamics and Earthquake Engineering (COMPDYN 2011), Corfu, Greece, May 25-28, pp. 25-28.

[42] *F. Villecco and A. Pellegrino*, Evaluation of Uncertainties in the Design Process of Complex Mechanical Systems, Entropy, 2017, 19, 475.

[43] *C. M. Pappalardo, M. Wallin and A. A. Shabana*, A New ANCF/CRBF Fully Parametrized Plate Finite Element, ASME Journal of Computational and Nonlinear Dynamics, 2017, 12(3), pp. 1–13.

[44] *M. C. De Simone, Z. B. Rivera and D. Guida*, Finite Element Analysis on Squeal-Noise in Railway Applications, FME Transactions, 2018, 46(1), pp. 93–100. doi:10.5937/fmet1801093D

[45] *F. Villecco and A. Pellegrino*, Entropic Measure of Epistemic Uncertainties in Multibody System Models by Axiomatic Design, Entropy, 2017, 19, 291.

[46] *M. C. De Simone and D. Guida*, Modal Coupling in Presence of Dry Friction, Machines, 2018, Accepted for publication

[47] *C. M. Pappalardo, Z. Yu, X. Zhang and A. A. Shabana*, Rational ANCF Thin Plate Finite Element, ASME Journal of Computational and Nonlinear Dynamics, 2016, 11(5), pp. 1–15.

[48] *C. M. Pappalardo, T. Wang and A. A. Shabana*, On the Formulation of the Planar ANCF Triangular Finite Elements, Nonlinear Dynamics, 2017, 89(2), pp. 1019-1045.

[49] *P. Sena, M. D'Amore, M. Pappalardo, A. Pellegrino, A. Fiorentino, and F. Villecco*, Studying the Influence of Cognitive Load on Driver's Performances by a Fuzzy Analysis of Lane Keeping in a Drive Simulation, IFAC Proceedings Volumes, 2013, 46(21), pp. 151-156.

[50] *X. Xu, T. Chen, L. Chen and W. Wang*, Longitudinal force estimation for motorized wheels driving electric vehicle based on improved closed-loop subspace identification, Journal of Jiangsu University (Natural Science Edition), 2016, 37(6), pp. 650–656.

[51] *A. Bouhenna, M. Chenafa, A. Mansouri and A. Valera*, Gantry robot control with an observer based on a subspace identification with multiple steps data, International Review on Modelling and Simulations, 2011, 4(6), pp. 3309–3316.

[52] *D. Guida and C. M. Pappalardo*, A New Control Algorithm for Active Suspension Systems Featuring Hysteresis, FME Transactions, 2013, 41(4), pp. 285–290.

[53] *D. Guida and C. M. Pappalardo*, Forward and Inverse Dynamics of Nonholonomic Mechanical Systems, Meccanica, 2014, 49(7), pp. 1547–1559.

[54] *A. Ruggiero, S. Affatato, M. Merola and M. C. De Simone*, Fem Analysis of Metal on Uhmwpe Total Hip Prosthesis During Normal Walking Cycle, Programme and Proceedings of the XXIII Conference of the Italian Association of Theoretical and Applied Mechanics (AIMETA 2017), 4-7.09.2017, Salerno, Italy, 2017, pp. 1885–1892

[55] *F. Sansone, P. Picerno, T. Mencherini, F. Villecco, A. M. D'Ursi, R. P., Aquino, M. R., and Lauro*, Flavonoid Microparticles by Spray-drying: Influence of Enhancers of the Dissolution Rate on Properties and Stability", Journal of Food Engineering, 2011, 103(2), pp. 188-196.

[56] *C. M. Pappalardo, Z. Zhang and A. A. Shabana*, Use of Independent Volume Parameters in the Development of New Large Displacement ANCF Triangular Plate/Shell Elements, Nonlinear Dynamics, Accepted for publication, DOI: https://doi.org/10.1007/s11071-017-4008-x.

[57] *A. Pellegrino, and F. Villecco*, Design Optimization of a Natural Gas Substation with Intensification of the Energy Cycle, Mathematical Problems in Engineering, 2010, 294102.

[58] *V. M. Cvjetkovic and M. Matijevic*, Overview of architectures with Arduino boards as building blocks for data acquisition and control systems, International Journal of Online Engineering, 2016, 12(7), pp. 10–17.

[59] *P. Škrabánek, P. Vodička and S. Yildirim-Yayilgan*, Control System of a Semi-Autonomous Mobile Robot, IFAC-PapersOnLine, 2016, 49(25), pp. 460–469.

[60] *D. Davis and P. Supriya*, Implementation of fuzzy-based robotic path planning, Advances in Intelligent Systems and Computing, 2016, 380, pp. 375–383.

[61] *B. Grămescu, C. Niţu, N.S.P. Phuc and C. I. Borzea*, PID control for two-wheeled inverted pendulum (WIP) system, Romanian Review Precision Mechanics, Optics and Mechatronics, 2015, 48, 246–251.